EXPERIMENTS AND ANALYSIS OF A COMPACT ELECTROTHERMAL THRUSTER

Jes Asmussen, Professor
Department of Electrical Engineering
Michigan State University
East Lansing, MI, USA 48824-1226

Stan Whitehair, Research Engineer
IBM, T.S. Watson Research Center
Yorktown Hts., NY, USA 10598

ABSTRACT

The description and experimental performance of a compact microwave electrothermal thruster (MET) are presented. This thruster makes use of a coaxial applicator to couple microwave power into a high pressure discharge. Unlike earlier experiments, it uses no fused quartz in the discharge chamber and the nozzle. This allows high temperatures in the discharge chamber without quartz erosion and melting, thereby improving thruster performance and lifetime. Further, the thruster design is compact, enhancing its potential as a space engine. Experimental tests using nitrogen and helium propellants with input powers levels of 200 W - 1.5 kW are presented. Experimental results, which produced energy efficiencies of 20-60% and specific impulse of 250-450 sec., compare favorably to previous experimental MET performance.

1.0 INTRODUCTION

The microwave electrothermal thruster (MET) is a relatively new electric engine concept that offers the promise of high performance and long lifetime at high levels of input power. Unique features of this electric engine concept are its ability to create a microwave arc-like discharge separated or floating away from any electrodes or enclosing walls. In addition, microwave energy can be transferred into the discharge with coupling efficiencies in excess of 95%. Because of these advantages the MET concept has been identified as a promising future high power electric thruster.[1]

Initial experimental investigations employed two basic microwave energy coupler (or applicator) concepts.[2-6] The earliest practical demonstration of the MET used a coaxial applicator to produce a 2.45 GHz high pressure discharge in nitrogen gas.[2,3] Input powers varied from 200 to 600 W as discharge pressured increased from 100 Torr to over one atmosphere and as the corresponding flow rates increased from 6.4×10^{-5} kg/s to 11.7×10^{-5} kg/s. Measured thruster energy efficiency varied between 30% to 60% and the specific impulse varied from 150-230 s.

Later experiments, which were tested with input microwave power levels from 500 - 2,000 W, employed a cylindrical cavity applicator to couple microwave energy into the discharge.[3-6] Again the discharge chamber and nozzle were made from a quartz tube located concentrically along the axis of the cavity. Microwave discharges were excited with either the TM_{012} or TM_{011} cavity modes in nitrogen and helium gases. Experimental performance in nitrogen gas[6] with flow rates as high as 146×10^{-6} kg/s and discharge pressures over one atmosphere resulted in thruster energy efficiencies of 10-25% and specific impulse as high as 280 s. Cavity experiments[4] with helium gas excited in the TM_{011} cavity mode resulted in energy efficiencies of 10-50% and a specific impulse of 200-600 s.

This experimentally measured performance compared favorably with other electrothermal thrusters. However, quartz nozzle melting and erosion limited the input power and specific impulse, and forced air cooling of the discharge chamber resulted in reduced efficiencies. Thus, it appeared that design improvements that incorporated higher-temperature nozzle materials and more efficient discharge chambers could yield improved performance.

More recent experiments[7-10] have been concerned with the use of metal nozzles and boron nitride discharge chamber/nozzle combinations. Preliminary experimental results[7,8,10] in nitrogen gas using quartz enclosed discharge chambers terminated with metal nozzles show that nozzle erosion and melting can be eliminated and specific impulse improved to 310-325 s. Experiments using boron nitride tubes and nozzles[9] have demonstrated that discharges can be maintained at the high pressures and flow rates required for thruster operation. However, more extensive experimental work is required to determine the usefulness of these configurations.

Each of the experimental discharge chambers[2-10] has either a quartz or boron nitride discharge chamber enclosing the discharge. The enclosing chamber, while separated from the hot discharge, is very close to thedischarge boundary and thus the wall is subjected to high heat fluxes from the discharge. As input power increases the discharge grows in size and radial heat transfer to the walls increases. In fact, at high input power levels the discharge may actually touch the walls resulting in increased power loss and increased wall erosion and melting. Thus, it is desirable that a high power MET not only use high temperature nozzle materials but also completely eliminate the enclosing discharge chamber walls.

This paper presents a description and experimental performance of redesigned coaxial MET. While this configuration was the first to demonstrate the MET concept it has not received as much experimental attention as the cavity applicator configuration. The coaxial applicator has been modified to remove the quartz tube and nozzle, and the brass applicator wall serves not only as a guide for the microwave energy, but also becomes the arc-stabilizing discharge chamber wall. A metal nozzle, similar to earlier designs,[3,7,8] is also incorporated into the applicator and a radial input gas flow produces a vortex flow through the discharge. The result is a cylindrical, compact (< 9 cm diameter and 12 cm long) coaxial MET that is capable of operation at much higher powers than earlier designs without nozzle and wall melting and erosion. The experimental results in nitrogen and helium gas presented here indicate the potential of this physically compact design to operate at high power levels.

2.0 DESCRIPTION OF THE COAXIAL APPLICATOR AND EXTERNAL MATCHING CIRCUIT

Figure 1 displays a quarter section isometric cutaway view of the MET together with an external matching circuit. The coaxial energy absorption chamber has been redesigned to remove the quartz discharge chamber and nozzle. Figure 2 displays an enlargement of just the energy absorption chamber with the microwave discharge ignited. As shown in these figures, components 5-17 make up the coaxial

energy absorption chamber and components 1-4 form the microwave input and external applicator coaxial matching circuits. It is important to observe that the coaxial applicator also serves as the discharge chamber. A further benefit of this new design is that the energy absorption chamber has been reduced in size to a length of 12 cm and an outside diameter of 9 cm. The various components of the MET and its external matching circuit are described in detail below.

The experimental thruster is composed of three distinct subassemblies. These subassemblies include parts for the external matching circuits and the energy absorption chamber or only components for the energy absorption chamber. As shown in Figure 1 the first subassembly consists of components 1-6. Input microwave power passes through a 1-5/8" (4.12 cm) EIA coaxial flange (3) and then enters a coaxial microwave tuning circuit formed by a 4.8 cm i.d. cylindrical brass outer conductor (1) and a 2 cm o.d. brass center conductor (2). A sliding short (4) serves as one tuning adjustment and the center conductor (2) is also independently adjustable. A teflon plug (5) seals the external matching network from the discharge chamber. Input gas enters through port (6), is distributed around the teflon plug by an annular distribution ring and enters the discharge chamber through holes drilled at angles across the center axis of the plug. This produces a vortex flow in the chamber and through the discharge helping to stabilize the discharge (8).

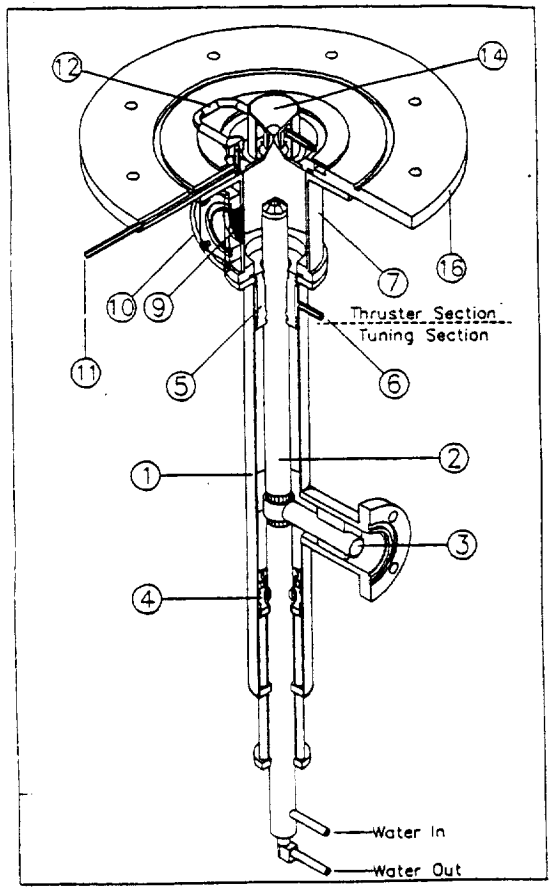

Figure 1. Isometric view of coaxial MET and external matching circuit.

A second subassembly consists of the cylindrical center portion of the discharge chamber. This subassembly is formed by a 6.5 cm i.d. by 10 cm long brass cylindrical section (7) which serves to guide the electromagnetic energy and contain and stabilize the microwave discharge. As shown in Fig. 2 the discharge (8) is formed along the center axis of this chamber and is attached to the tip of the center conductor (2). The tip is made of inconel and is silver soldered to the center conductor and is cooled by water flowing through a long 35 cm tube located inside and along the center axis of the canter conductor (2). A screen viewing window (9) and a plexy glass window (10) allow the visual monitoring of the discharge while sealing the discharge chamber from atmospheric air.

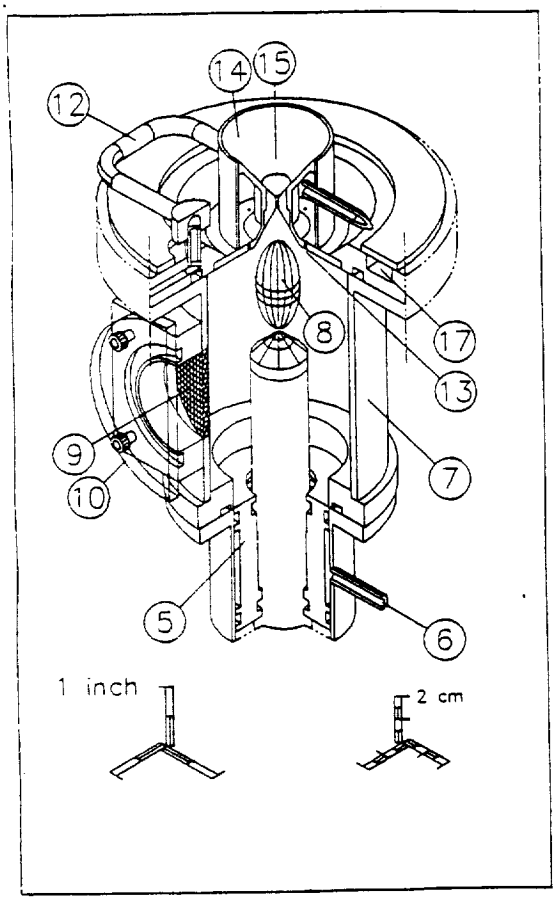

Figure 2. Enlarged isometric view of the the coaxial MET with the vacuum flange and matching circuit removed.

The third subassembly is a stainless-steel nozzle/baseplate that was also used with the cavity applicator.[3,7-9] Gas enters through the input port (11) and is distributed evenly by a gas flow system (12) that helps to cool the nozzle and preheat the input gas. The gas is injected into the discharge chamber via a circle of eight equally spaced small holes (13) and after passing through the discharge region exits via the nozzle (14) and nozzle insert (15). The nozzle insert allows different nozzle materials and shapes to be tested. As shown in Figure 1 a large vacuum plate (16) attaches the applicator to the vacuum system. The vacuum plate is sealed to the discharge chamber by an O-ring and the plate is kept cool by a water cooling channel (17).

Figure 3 displays the equivalent circuit of the coaxial matching system. In contrast to the cylindrical cavity applicator thruster, where impedance matching is achieved through variation of the cavity size and coupling probe position, im-

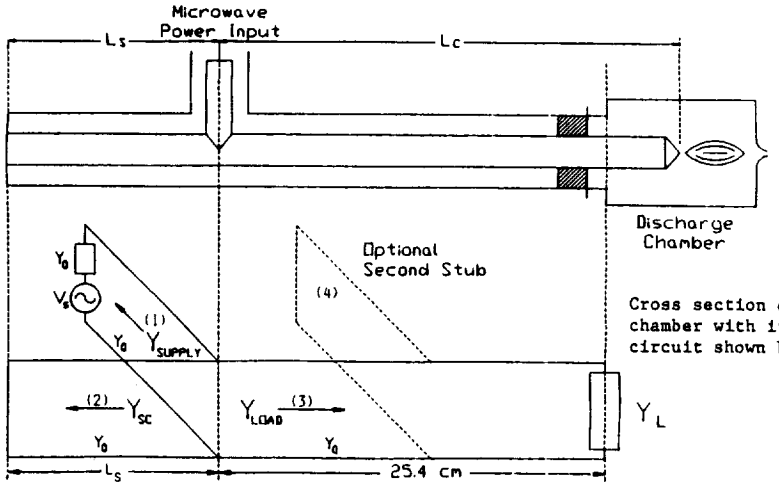

Figure 3.

Cross section of tuning circuit and absorption chamber with its equivalent transmission line circuit shown below.

pedance matching in this device takes place external to the thruster (or external to the energy absorption chamber). As shown in Figure 3 the external matching circuit consists of a shorted coaxial cable (2) with a variable length L_s and a coaxial section (3) of fixed length ℓ = 25.4 cm. These two coaxial sections join in parallel with the coaxial input coaxial circuit (1) which in turn is connected to the microwave power generator, microwave power measuring system and circulator.

As shown in Figure 3 the equivalent circuit consists of three transmission line sections connected in parallel. This type of transmission line equivalent circuit representation has been extensively discussed in many References.[1,2] In the circuit models developed here it is assumed for simplicity that the three lines are lossless even though in an actual experiment microwave energy is deposited in the coaxial conductors by the standing wave fields inside the lines. The input transmission line (1) represents the input power system and associated coaxial cable. Since the power source is matched by the circulator it is represented by an ideal voltage generator matched to the transmission line with an internal admittance equal to the line characteristic admittance, Y_o, of .02 mhos. The admittance of the shorted transmission line (2) at the T joint can be represented as

$$Y_{sc} = -jY_o \cot\beta L_s = +jB_{sc}(L_s) \qquad (1)$$

where Y_{sc} = the input admittance,
Y_o = characteristic admittance of the line,
L_s = length of the line,
λ = wavelength of the electromagnetic energy,
β = propagation constant of the transmission line = $\frac{2\pi}{\lambda}$.

It is useful to note that this admittance (neglecting line losses) is a pure susceptance and can vary over a very wide range of both capacitive and inductive susceptances depending on the line length L_s.

The equivalent admittance of the energy absorption chamber is represented as Y_L. In general Y_L will have a real and an imaginary part representing respectively the losses of the discharge and the reactive effects of the electromagnetic fields in the applicator and in the discharge. Again using the equivalent transmission line representation this load will be reflected (neglecting effects of the teflon plug) to the T joint as the following input admittance.

$$Y_{LOAD} = Y_o \frac{Y_L + jY_o \tan\beta\ell}{Y_o + jY_L \tan\beta\ell} = G_1 + jB_1 \qquad (2)$$

Thus, the conductance and susceptance at ℓ = 25.4 cm due to the thruster will have a real and imaginary part which are functions of Y_L.

In order to produce an impedance match at the T joint

$$Y_{in} = Y_{sc} + G_1 + jB_1 = Y_o \qquad (3)$$

$$= +jB_{sc}(L_s) + G_1 + jB_1 = Y_o$$

Y_o is fixed and real thus equation (3) shows that the best match that can be achieved is when the susceptances cancel; i.e. when

$$+jB_{sc}(L_s) = -jB_1 \qquad (4)$$

Since the length ℓ is fixed this occurs when L_s is varied until equation (4) holds. Then

$$Y_{in} = G_1 \qquad (5)$$

In general G will not equal Y_o and thus this single stub matching system will not match all discharge loads. As is noted when discussing the experimental results, this is observed experimentally. The addition of an extra short circuit stub or stubs (an extra stub is shown as the dashed transmission line (4) in Fig. 3) would have the benefit of allowing a wider range of discharge loads to be matched but has the disadvantage of increasing tuning complexity and increasing matching circuit losses. Thus, the experimental thruster uses a non-optimal but simple matching circuit.

3.0 EXPERIMENTAL SYSTEMS

The experimental systems employed were similar to those used in earlier experiments.[3-7] In particular the microwave systems consisted of 1) 2.45 - GHz, CW, variable-power (0 - 2500 W) source, 2) a circulator and matched dummy load, 3) waveguide directional couplers, attenuators and power meters that measure incident power P_i and reflected power P_r, 4) a 1 5/8" coaxial input coupling system and 5) the coaxial microwave applicator and external matching circuits. The power $P_t = P_i - P_r$ represents the sum of the power absorbed in the external matching circuits P_c and the power absorbed in the

applicator (energy conversion chamber). The power coupled into the applicator then divides between the power P_b absorbed by the conducting walls and the power absorbed by the discharge P_a. Thus $P_t = P_i - P_r = P_a + P_b + P_c$.

As the experimental conditions vary P_t is measured as the difference between incident and reflected power meters while P_b and P_c cannot be measured directly. In fact, for different input powers, pressures and gas flow conditions, P_b and P_c can vary considerably even if P_t is held constant. From measurements made in cylindrical cavity experiments[3-7] it is expected that $P_b \ll P_a$, i.e., the applicator coupling efficiency is > 95%. For certain discharge load conditions P_c can become a significant fraction of the total input power P_t. Since P_b and P_c cannot be determined for the experiments reported here, the power absorbed in the discharge will be assumed to be equal to P_t when calculating the overall energy. This has the effect of producing lower calculated energy efficiencies.

Experiments were performed using nitrogen and helium gases as propellants. A two channel flow controller maintained a constant flow rate as gas flow was varied between inputs (6) and (11). An electric monometer and a Heise gauge measured discharge pressure. The thruster and coaxial matching circuits were positioned vertically and connected to a vacuum chamber formed out of 6" pyrex glass tubing. This vacuum chamber included a heat exchanger to cool the exhausted propellant protecting the vacuum system from the high temperature propellant.

The vacuum was produced by a two stage mechanical roughing pump, and a gate valve allowed the pump to be shut off from the discharge chamber evacuation line. The specific impulse, energy efficiency and the power to thrust ratio were calculated from equations (1)-(9) of Reference 4. These quantities were determined by the indirect thrust method where the hot and cold discharge chamber pressures are measured under constant flow conditions. This method, which is described in detail in References 3 and 4, requires that the nozzle is operated in a choked condition, i.e., the pressure downstream from the nozzle must be held below one Torr.

4.0 EXPERIMENTAL RESULTS

A discharge was ignited by first adjusting the center conductor length L_c to the approximate desired position and reducing the input gas flow to allow the pressure in the discharge chamber to drop to approximately one Torr. Input microwave power was increased to over 100 W and the input gas flow was increased while the sliding short was adjusted for minimum reflected power. The discharge was then ignited after which the gas flow and input power were adjusted to the desired operating conditions, and L_s and L_c were also readjusted to the best match or minimum reflected power. Since the best experimental results were obtained with no gas flow into input (11) all experimental data presented here had the input gas flowing entirely through input (6) (see Fig. 1).

Optimal L_s and L_c were determined experimentally. For a given gas and input power L_c was adjusted to provide a good energy efficiency and specific impulse. L_s was adjusted to yield the best match for a given set of operating conditions. Excellent matching was achieved for low incident powers ($\leq$ 600 W). However as input power was increased beyond 600 W the applicator matching became more difficult until at approximately 1.5 kW any further increase in incident power was entirely reflected. As indicated earlier the difficulties of matching this applicator are concerned with the single stub matching and do not represent a limitation of this applicator geometry.

Experimental runs were performed by establishing a desired propellant flow rate and holding this flow rate constant throughout the entire experimental run. Once the desired flow rate was achieved, the cold discharge pressure, p_c, was measured. The discharge was then ignited and the input microwave power was adjusted to the desired level. The applicator input power, P_t, and the steady state discharge pressure, p_H, were measured for several operating points as the input power, P_t, was varied. After each experimental run, the discharge chamber was allowed to cool back to the initial conditions as a check against nozzle degradation. The energy efficiency, specific impulse and the thrust-to-power ratio were calculated from Eqs. (5-7) and (9) of Reference 4. Figures 4-7 summarize typical experimental results in nitrogen and helium gas. The experimental conditions for the data points shown in these figures are listed in Table 1.

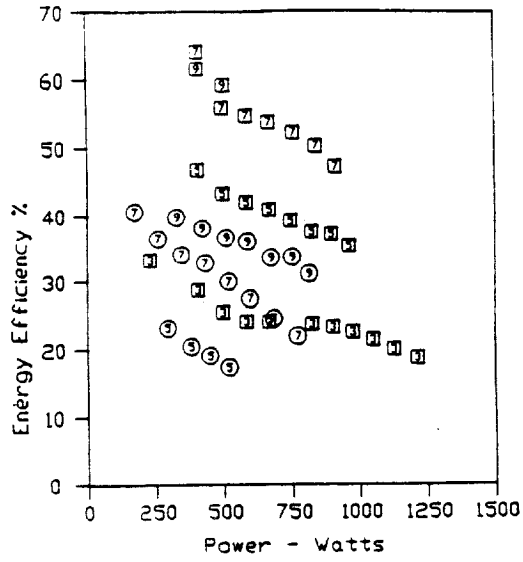

Figure 4
Energy efficiency versus input microwave power for different experimental conditions in Table 1. Note that the square data points denote nitrogen gas and the round points denote helium. Numbers in the center denote the different flow rates listed in Table 1.

Seven typical experimental runs for helium and nitrogen gases are summarized in Table 1. As shown, experimental data was taken for preset constant-input gas flow and L_s and L_c conditions as the input power was continuously increased from a low initial value. Data points for each of the seven conditions are displayed in Figs. 4-6. Specifically the calculated energy efficiencies vs input power are displayed in Fig. 4. The specific impulse and thrust to power ratio were calculated for each data point shown in Fig. 4 and are displayed in Figs. 5 and 6. Figure 7 compares the coaxial experimental data of Fig. 5 to earlier

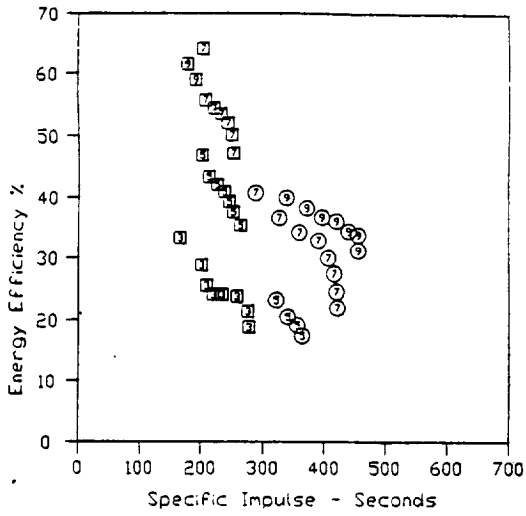

Figure 5. Energy efficiency versus specific impulse for different conditions listed in Table 1.

#	Point	Gas Type	Flow Rate ($kg/s \times 10^{-6}$)	Discharge Pressure (Torr)	Nozzle Size (Diameter)	L_s cm	L_c cm
1.	3	N_2	62.5	530-888	1.02mm	8.6-8.7	30.8
2.	5	N_2	104	1057-1385	1.02mm	8.5-8.9	32.2-32.3
3.	7	N_2	146	1450-1890	1.02mm	8.2-8.3	30.8-31.0
4.	9	N_2	187	1800-1936	1.02mm	8.6-8.7	30.8
5.	5	He	14.9	325-368	1.02mm	8.25-8.3	32.4
6.	7	He	20.8	410-599	1.02mm	8.25-8.3	32.4
7.	9	He	26.8	576-865	1.02mm	7.9-8.45	31.9-32.5

Table 1. Operating conditions for experiments with a compact microwave electrothermal thruster using helium and nitrogen propellant.

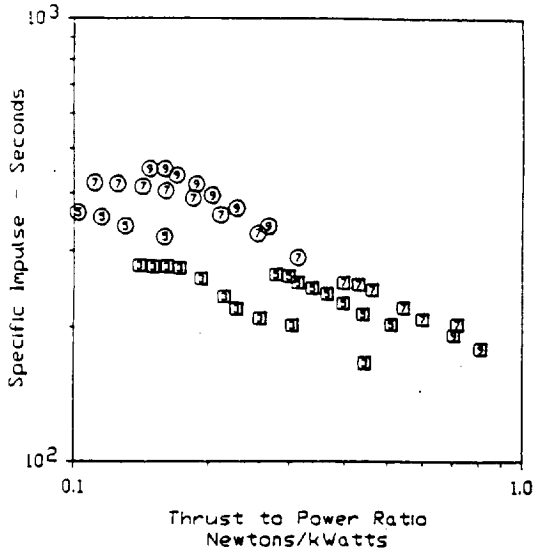

Figure 6. Specific impulse versus thrust to power ratio for experimental conditions listed in Table 1.

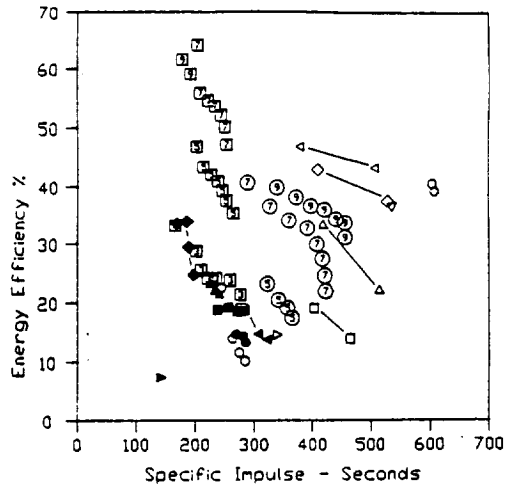

Figure 7. Figure 5 compared with data from Figure 6 in Reference 4 and Figure 7.7 in Reference 3.

experiments using quartz nozzles and cavity applicators. The cavity applicator data was taken from Fig. 7.7 in Reference 3 and Fig. 6 in Reference 4.

Experimental data indicates that the performance is similar to that of earlier experiments with cavity applicators. In fact, energy efficiencies in nitrogen exceed those measured in earlier experiments despite the water cooling of the nozzle and including the coupling losses of the external matching circuit. Specific impulse, despite being limited by input power coupling problems is also good considering the high flow rates.

5.0 DISCUSSION

The experimental performance of this redesigned coaxial MET shows that it is possible to operate a MET without an arc stabilizing quartz or dielectric discharge chamber and nozzle. The applicator walls were reduced to a diameter which was below cutoff for ordinary empty waveguide TE and TM electromagnetic modes. Thus these experiments demonstrate that discharge formation is possible inside a cylindrical metal tube which does not allow the usual empty waveguide propagating electromagnetic fields to exist. Experimental performance was comparable to or better than other configurations without quartz tube or nozzle melting and erosion. Operation in helium and nitrogen gases for 30 hours showed no signs of nozzle or center conductor deterioration. The lack of discharge chamber wall cooling produced high energy efficiencies even though the center conductor was water cooled.

The resulting design is a compact, cylindrical 9 cm diameter by 12 cm long engine that has operated at 1.5 kW power levels. Higher input powers are possible and will be investigated in later experiments. It is expected that the small physical size together with the ability to handle high input powers will make this MET attractive for space applicators.

Further improvements of this concept are possible. Besides redesigning for higher power operation they are concerned with improving the matching, removing the water cooling from the center conductor and a further reduction and optimization of the physical size for different levels of rated input power. The improved matching could be solved by one or two additional, properly placed coaxial tuning stubs.

While this would match the MET to the transmission line for a wider range of discharge loads it would also add to the complexity of operation and may add significantly to the system circuit losses. A different but potentially simpler and more efficient matching approach would be to employ the internal tuning as is described in other plasma applicator systems. All tuning would take place inside the applicator[4,13,14] and thus would not add additional significant losses.

The use of water cooling in this thruster, especially in the center conductor, could be considered a drawback for potential space use. However, in this prototype design water cooling is used to protect the o-rings and solder joints. Any thruster designed for use in space would be constructed with welded joints eliminating the need for this cooling. In addition, if some of the propellant is passed through the center conductor and through the tip, the propellant will act as a coolant itself and thus it may be possible to operate this thruster with the discharge in contact with the tip without additional cooling. Finally, with improved understanding of the discharge and the electromagnetic field patterns inside the thruster it may be possible to move the discharge completely off the center conductor.

6.0 REFERENCES

1. Byers, R.C., "The NASA Electric Propulsion Program, " AIAA Paper, 87-1098, 1987.

2. Whitehair, S., Asmussen, J., and Nakanishi, S., "Demonstration of a New Electrothermal Thruster Concept," Applied Physics Letters, Vol. 44, May 1984, pp. 1014-1016.

3. Whitehair, S., "Experimental Development of a Microwave Electrothermal Thruster," Ph.D. Dissertation, Michigan State University, 1986.

4. Whitehair, S., Asmussen, J., and Nakanishi, S., "Microwave Electrothermal Thruster Performance in Helium Gas," Journal of Propulsion and Power, Vol. 3, March-April 1987, pp. 136-144.

5. Asmussen, J. and Whitehair, S., "Performance Measurements on a Microwave Electrothermal Engine," presented at the 1984 IEEE International Conference on Plasma Science, St. Louis, MO, May 14-16, 1984.

6. Asmussen, J., Whitehair, S., and Nakanishi, S., "Experiments with a Microwave Electrothermal Thruster Concept," AIAA/JSASS/DGLR 17th International Electric Propulsion Conference, IEPC 84-74, Tokyo, Japan, May 1984.

7. Whitehair, S., Asmussen, J. and Nakanishi, S., "Recent Experiments with Microwave Electrothermal Thrusters," AIAA Paper, 85-2051, 1985.

8. Whitehair, S., Frasch, L. and Asmussen, J., "Experimental Investigation of Microwave Electrothermal Thruster Configurations," presented at the 13th IEEE International Conference on Plasma Science, Saskatoon, Saskatchewan, Canada, 1986.

9. Whitehair, S., Frasch, L. and Asmussen, J., "Experimental Performance of a Microwave Electrothermal Thruster with High Temperature Nozzle Materials," AIAA Paper, 87-1016, 1987.

10. Herlan, W. and Jassowski, D., "Microwave Thruster Development," AIAA Paper, 87-2123, 1987.

11. Mallavarpu, R., Asmussen, J., and Hawley, M.C., "Behavior of a Microwave Cavity Discharge over a Wide Range of Pressures and Flow Rates," IEEE Transactions on Plasma Science, Vol. PS-6, Dec. 1978, pp. 341-354.

12. Collin, R.E., "Foundations for Microwave Engineering," McGraw-Hill Book Co., New York, 1966, pp. 203-229.

13. Asmussen, J., Mallavarpu, R., Hanann, J.R. and Park, H.C., "The Design of a Microwave Plasma Cavity," Proceedings of the IEEE, Vol. 62, Jan. 1974, pp. 109-117.

14. Root, J. and Asmussen, J., "Experimental Performance of a Microwave Cavity Plasma Disk Ion Source," Review of Scientific Instruments, Vol. 56, Aug. 1985, pp. 1511-1519.

7.0 ACKNOWLEDGMENTS

This work was supported in part by NASA Grant NAG-3-305.